AGU PUBLICATIONS

Geophysical Research Letters

RESEARCH LETTER
10.1002/2016GL070370

Key Points:
- We analyzed the geomorphology several flows of craters to prove if they were formed by impact melt or cryovolcanic processes
- The low coefficient of friction implies higher flow efficiency for flows on Ceres than for similar features on other planetary bodies
- The formation of the flows could be due to the mobility of crustal subsurface reservoirs enriched with hydrated salts by impacts

Correspondence to:
K. Krohn,
katrin.krohn@dlr.de

Citation:
Krohn, K., et al. (2016), Cryogenic flow features on Ceres: Implications for crater-related cryovolcanism, *Geophys. Res. Lett.*, *43*, doi:10.1002/2016GL070370.

Received 11 JUL 2016
Accepted 15 NOV 2016
Accepted article online 17 NOV 2016

Cryogenic flow features on Ceres: Implications for crater-related cryovolcanism

K. Krohn[1], R. Jaumann[1,2], K. Stephan[1], K. A. Otto[1], N. Schmedemann[2], R. J. Wagner[1], K.-D. Matz[1], F. Tosi[3], F. Zambon[3], I. von der Gathen[1], F. Schulzeck[1], S. E. Schröder[1], D. L. Buczkowski[4], H. Hiesinger[5], H. Y. McSween[6], C. M. Pieters[7], F. Preusker[1], T. Roatsch[1], C. A. Raymond[8], C. T. Russell[9], and D. A. Williams[10]

[1]Institute of Planetary Research, Deutsches Zentrum für Luft- und Raumfahrt, Berlin, Germany, [2]Institute of Geological Sciences, Planetary Sciences and Remote Sensing, Freie Universität Berlin, Germany, [3]INAF-IAPS, National Institute for Astrophysics, Rome, Italy, [4]The Johns Hopkins University Applied Physics Laboratory, Laurel, Maryland, USA, [5]Institute of Planetology, Westfälische Wilhelms-Universität Münster, Münster, Germany, [6]Department of Earth and Planetary Sciences, University of Tennessee, Knoxville, Tennessee, USA, [7]Brown University, Providence, Rhode Island, USA, [8]Jet Propulsion Laboratory, California Institute of Technology, Pasadena, California, USA, [9]Institute of Geophysics and Planetary Physics, University of California, Los Angeles, California, USA, [10]School of Earth & Space Exploration, Arizona State University, Tempe, Texas, USA

Abstract Craters on Ceres, such as Haulani, Kupalo, Ikapati, and Occator show postimpact modification by the deposition of extended plains material with pits, multiple lobate flows, and widely dispersed deposits that form a diffuse veneer on the preexisting surface. Bright material units in these features have a negative spectral slope in the visible range, making it appear bluish with respect to the grey-toned overall surface of Ceres. We calculate the drop height-to-runout length ratio of several flow features and obtain a coefficient of friction of < 0.1: The results imply higher flow efficiency for flow features on Ceres than for similar features on other planetary bodies with similar gravity, suggesting low-viscosity material. The special association of flow features with impact craters could either point to an impact melt origin or to an exogenic triggering of cryovolcanic processes.

1. Introduction

After orbiting asteroid Vesta between 2011 and 2012, NASA's Dawn spacecraft entered orbit around dwarf planet Ceres in March 2015 [*Russell et al.*, 2015]. The mission goals at Ceres are to characterize the geology, elemental and mineralogical composition, topography, shape, and internal structure of Ceres in order to understand its geological evolution [*Russell and Raymond*, 2011]. Smooth plains that cover the interior of a number of impact craters are one of the most prominent geological features on Ceres. Notable examples are Haulani, Kupalo, Ikapati, and Occator craters. Besides smooth plains, the geology of these craters is characterized by ponded material, flows with lobate flow fronts, and pits. Dawn Framing Camera (FC) data (monochrome and color ratio images) [*Sierks et al.*, 2011] from the high-altitude mapping orbit (HAMO), with a spatial resolution of 140 m/pixel, and from the low-altitude mapping orbit (spatial resolution of 35 m/pixel), as well as a HAMO Digital Terrain Model (DTM) [*Preusker et al.*, 2016] (135 m/pixel), were used to analyze smooth plains units and its associated features. A bluish signature can be seen for all investigated features in the enhanced FC HAMO color mosaic of the filters 5 (956 nm), 2 (555 nm), and 8 (440 nm) [*Pieters et al.*, 2016]. The potential presence of ice within Ceres' crust [*McCord and Sotin*, 2005] raises the prospect of geological processes similar to those on differentiated icy bodies [*Thomas et al.*, 2005]. Pre-Dawn telescopic observations suggested some aqueous alteration on Ceres, including the formation of clay-like materials [*Rivkin et al.*, 2011] and possibly salts covered by a regolith layer having only small-scale compositional variations [*Castillo-Rogez and McCord*, 2010; *McCord and Sotin*, 2005]. Thermal models suggest that Ceres is at least partially differentiated and could have undergone tectonic and cryovolcanic processes [*Castillo-Rogez and McCord*, 2010; *McCord et al.*, 2011]. Another possibility for the formation of flows on planetary bodies is impact melt. Impact melt normally occurs as lobate tongues of melt rocks near the crater rim or inside craters and is morphological similar to terrestrial lava flows. In this paper, we will discuss both processes to explain the formation of the flows on Ceres.

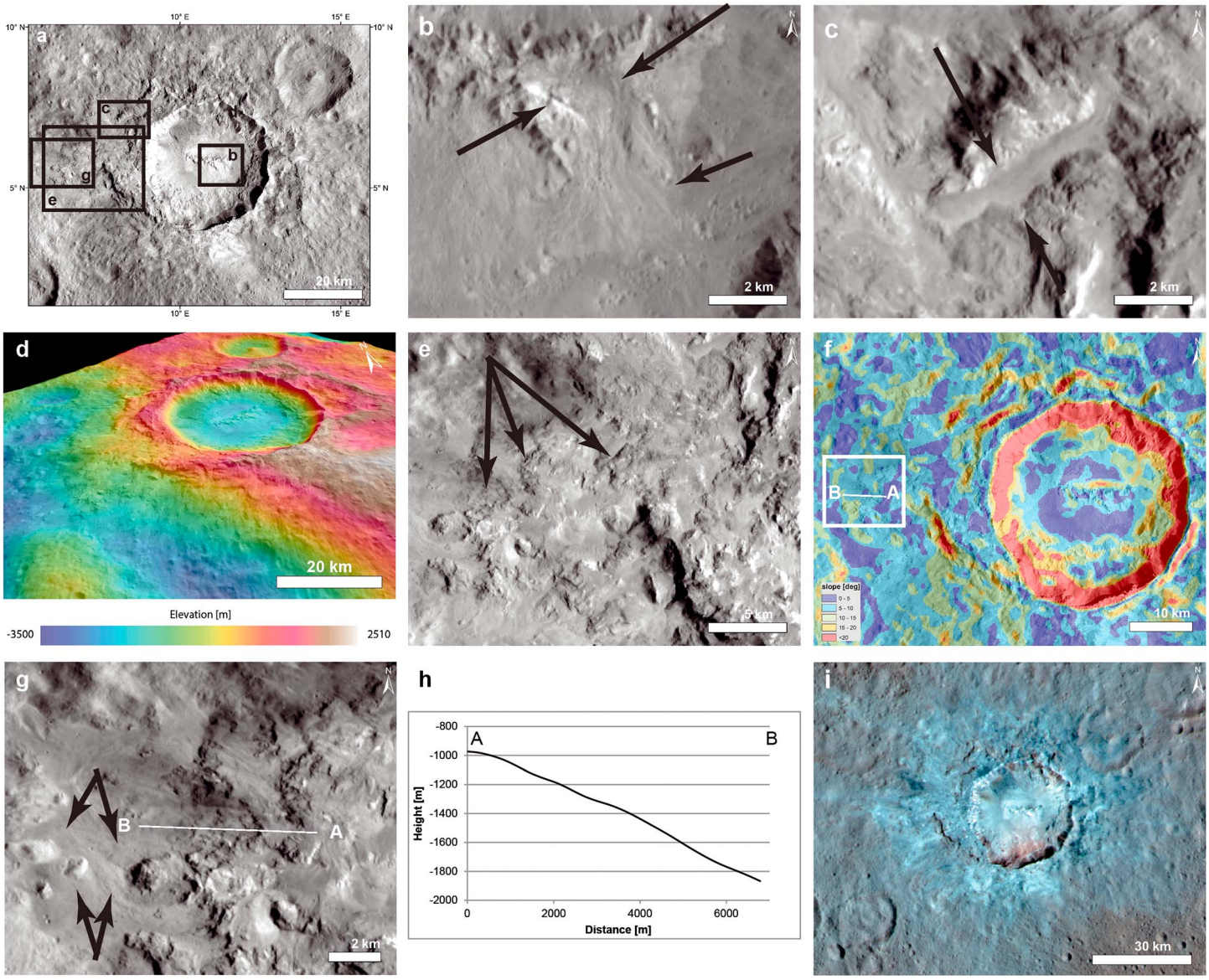

Figure 1. (a) Haulani crater. (b) Mountainous central region with flow (arrows). (c) Well-defined smooth lobes (arrows). (d) Three-dimensional view showing scarps bounding multiple flows in the west. (e) Multiple flow stages (arrows). (f) Slope map showing a shallow crater flank interrupted by scarps. White box shows the profile location. (g) Detailed view of multiple flows along the profile. Arrows mark streamlines around blocks. (h) Profile of flows showing a shallow crater flank. (i) Enhanced color mosaic.

2. Observations

2.1. Haulani

Haulani crater (Figure 1) exhibits interior smooth plains with flow features originating from a hummocky elongated mountainous ridge in the center, ponding toward mass-wasting deposits of the rim. One example exhibits a channel, stream lines, lobes, and a well-defined flow front (Figure 1b). The smooth crater floor is laced by pits. Some pit crater chains in the northwestern part are oriented parallel to the rim [*Krohn et al.*, 2016]. The pits lack raised rims and are located on the crater floor, predominately in clusters. The largest cluster is located north of the ridge with a maximum length of ~10 km and a maximum width of ~3.8 km. Smaller clusters are circumferential to the ridge but are absent in the eastern part, where mass-wasting deposits from the rim may have covered the pits. A small cluster of pits is located in the middle of the prominent ridge flow. The pits range in size from ~35 m (at the limit of resolution) to ~230 m in diameter.

Additional clusters of pits are detected in Haulani's southeastern to western ejecta blanket. These pits reach a maximum diameter of ~540 m.

Haulani shows several flow features running from the crater rim outward to the surrounding area, covering the preexisting surface. We can distinguish four types of flows: The first flow type (1) is defined by smooth lobes with well-defined margins and a very smooth featureless surface (Figure 1c). The lobes follow local depressions and range in length from 0.5 to 20 km and in width from 0.35 to 8.1 km. Most flows occur as narrow lobes, but we also found dilated flows streaming around solid blocks. Some of the narrow lobes contain channels following the flow direction. Additionally, flows near the crater rim show evidence for cracking. This flow type is predominantly distributed on the western and eastern crater flank but is less common on the northern crater flank. The second flow type (2) occurs as more viscous flows with a relatively smooth surface. These flows show clear margins of multiple flow stages on top of each other and occur only on the western crater flank, extending to a distance of up to 29 km from the rim and covering an area of about 945 km^2 (Figures 1d and 1e). Figure 1h shows a shallow crater flank with no evidence of terraces which had been overflowed by material. The third flow type (3) shows a very smooth but streaky surface with smooth material. The flows are affected by small narrow channels. This type is located on the central ridge flanks within Haulani as well as on the southern and northeastern crater flanks of Haulani. The last flow type (4) shows a relatively smooth surface interrupted by knobs. This type is located close to the crater rim on the northern and eastern crater flank of Haulani.

Haulani was formed on a topographic boundary. The eastern side is topographically elevated whereas the western side is lower (Figure 1d). The western side is affected by a broken crater rim, showing thin rock layers on the inner crater wall and multiple scarps, cracks, and shear zones outside the crater. The collapsed crater rim merges into the type 2 flows. These flows are bound by steep scarps related to the broken crater rim.

2.2. Kupalo

The crater floor of Kupalo reveals different complex processes. Like Haulani, Kupalo has a central ridge with lobate flow features, which seem to originate from the ridge crest. Furthermore, the ridge exhibits a smooth dome-like structure superimposing the ridge material with younger flows (Figure 2b). A second ridge in the south also exhibits some lobate flows running down to the crater floor as well as a dome-like structure. The crater floor is covered with plains of smooth ponded material, which partly covers the mass-wasting deposits originating from the steep crater walls in the north and east part. A huge lobate flow at the southwestern floor seems to originate from the southern crater floor and extends toward the crater wall (Figure 2b).

The crater floor is associated with pit crater chains, clusters of pits, and cracks. The northern crater rim shows some flows occurring inside and outside of the crater rim. They originated from small domes at the rim crest (Figure 2f). Compared to other peaks on the crater floor, the domes are topographically higher and reveal a conical shape with a very smooth surface.

The crater flanks contain smooth lobes with well-defined margins, ranging from 3.5 to 19 km in length and from 0.8 to 3.2 km in width. Some flows contain channels in flow direction (Figure 2d). Like Haulani, Kupalo was formed on a topographic boundary, showing a less intact crater rim with multiple fractures in the south and west, which are bound by steep scarps (Figure 2c).

2.3. Ikapati

Ikapati impacted half into a topographic high and half into a possible ancient basin showing a sharp crater rim in the north and east and a degraded one in the south and west (Figure 3c). Terraced mass-wasting material, originating from the sharp rim, fills nearly half of the crater floor in northeast direction. The other half of the crater floor consists of smooth material, interrupted by pitted terrain (Figure 3d), pit crater chains, and cracks. Ikapati shows smooth plains (Figure 3f) at different topographic levels associated with pits and well-defined lobate flow-like features that overran the degraded crater rim (Figure 3b). These flows originated from the crater rim and ran radially outward. They occur as relatively short narrow channelized lobes. Compared to the smooth plains material, the flows seem to be thicker and less smooth. The material forming the plains ponded in depressions and smaller craters southwest of Ikapati and covers the preexisting surface.

2.4. Occator

The interior of Occator exhibits extended plains of ponded material. The plains material is superposed on the mass-wasting deposits originating from the steep crater walls, leaving only the tops of the source blocks as

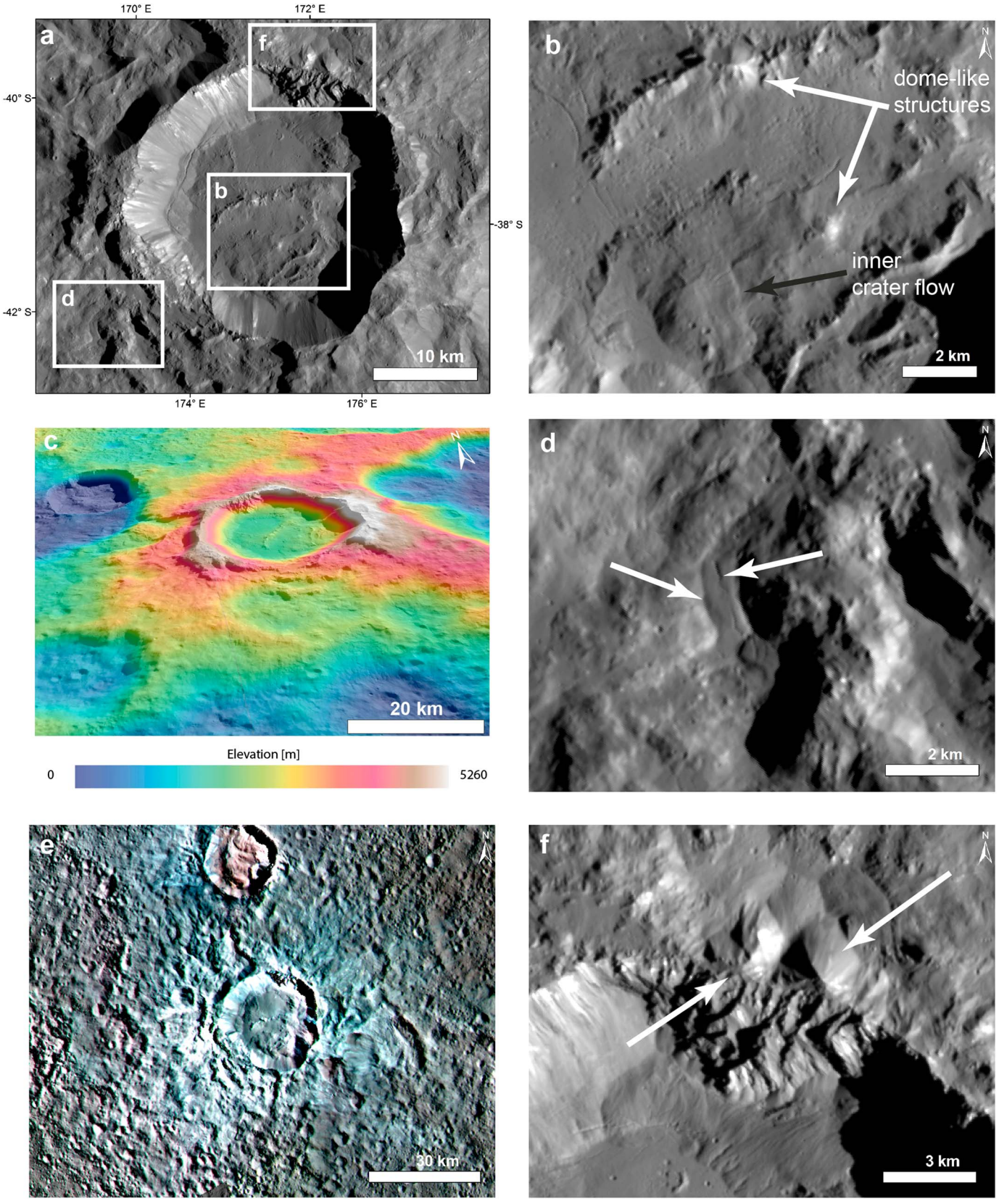

Figure 2. (a) Kupalo crater. (b) Crater floor with dome-like structures and flows (white arrows) and an inner crater flow (black arrow). (c) Three-dimensional view showing flows bound by scarps. (d) Well-defined smooth channelized lobes. (e) Enhanced color mosaic. (f) Domes with flows at crater rim.

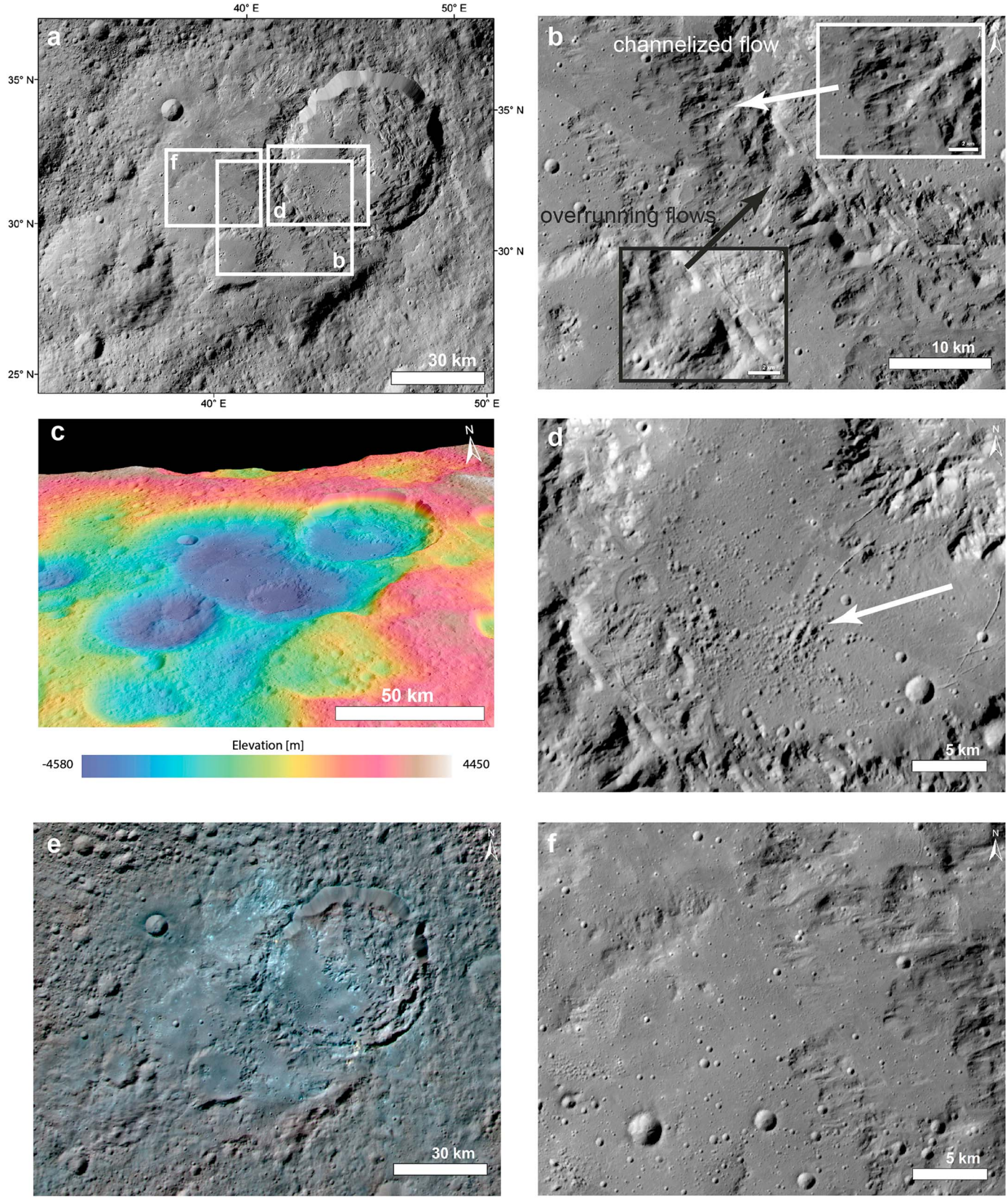

Figure 3. (a) Ikapati crater. (b) Flows override the SW rim (black arrow), closeup of channelized flow. (c) Three-dimensional view showing the topographic boundary. (d) Smooth inner crater plains contain collapse pits (arrow). (e) Enhanced color mosaic. (f) Smooth plains inside the adjacent depression.

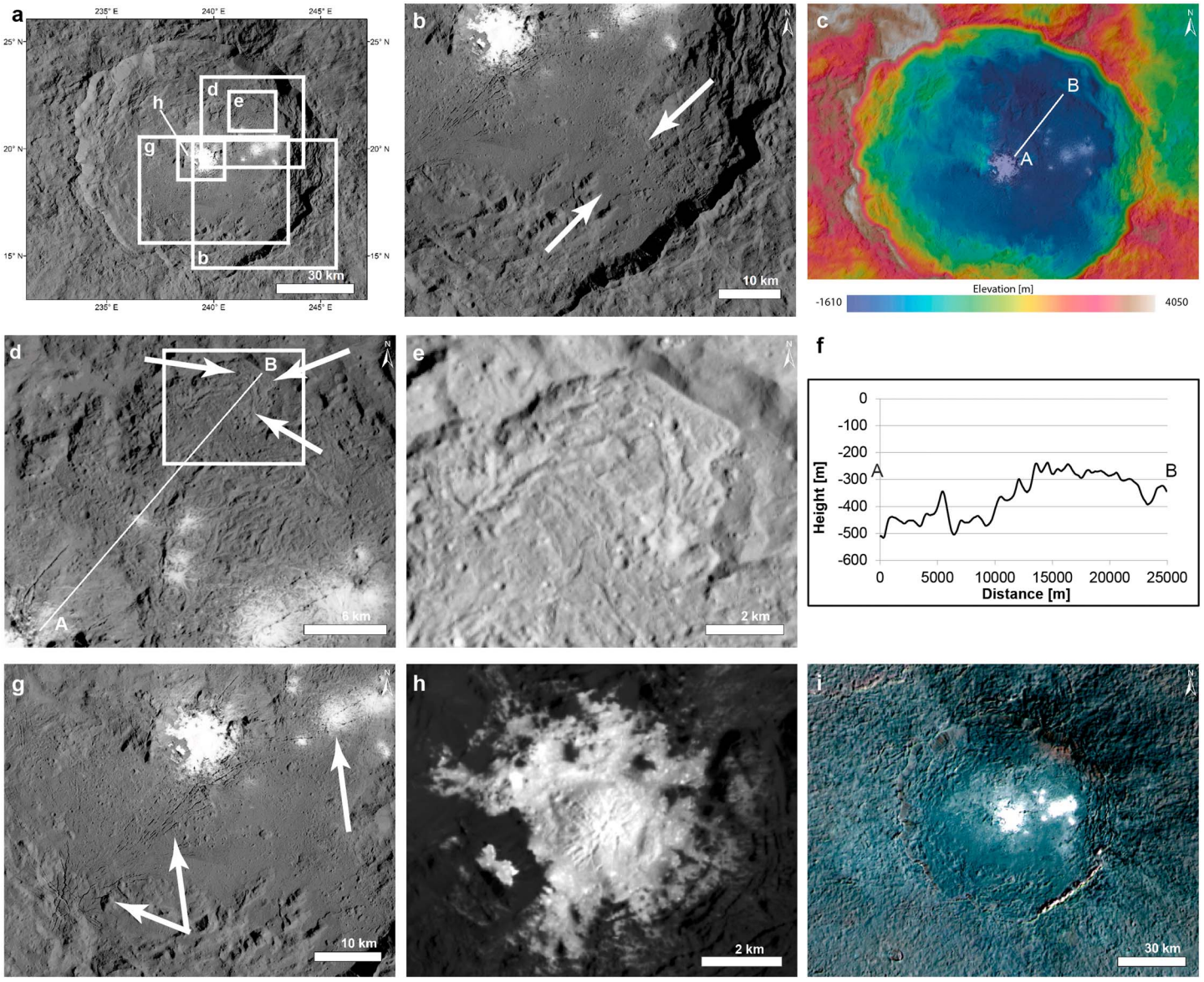

Figure 4. (a) Occator crater. (b) Plains of ponded material cover mass-wasting deposits and pileup at crater walls (arrows). (c) DTM showing the profile location. (d) Flows spread out from central white spot, and flow fronts collide with mass-wasting deposits; superimposed individual flows (arrows) indicate multiple flow events. Box shows location of Figure 4e. (e) Detailed view of individual flows showing a ropey surface. (f) Profile of crater floor, showing the upward direction of the flows. (g) Extension cracks extending from a hummocky area between flooded slumping blocks and spreading radially. (h) Higher stretch of bright dome showing the cracks on top. (i) Enhanced color mosaic.

isolated remnants and partly banking at the steep crater walls (Figure 4b). Toward the northeast, flows spread out from the central region associated with a bright dome, which is affected by radial cracks (Figure 4g). The center of Occator is dominated by bright material (Figure 4a) [*De Sanctis et al.*, 2015; *Nathues et al.*, 2015]. The western part of the central region is topographically elevated. The eastern part, mostly covered by bright material, is a depression with the small dome in its center (Figures 4c and 4h). The flows to the northeast appear to originate from the central bright region and move slightly uphill, ponding against rim-related mass-wasting deposits. These flows show at least three individual lobate flow surfaces superposed on each other, indicating multiple flow events (Figures 4d and 4e). This implies either a feeding source through a vent or a collapse of a bulged source region after it emptied.

Crater densities on Occator's floor are lower than those on the ejecta blanket, indicating a postimpact formation age of the flows [*Neesemann et al.*, 2016]. Occator shows radial extension cracks in its southwestern part,

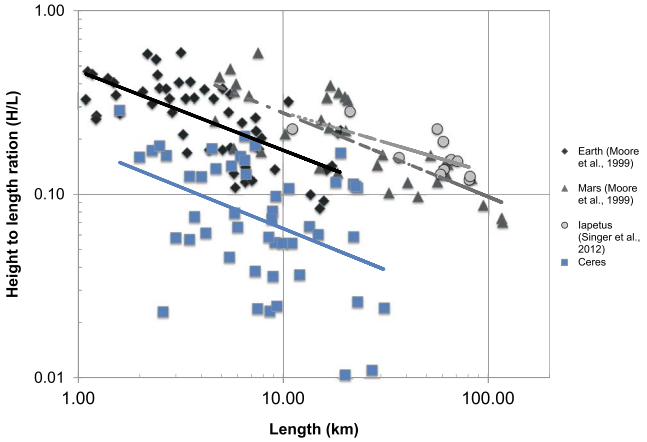

Figure 5. Plot of Cerean flows height over length (*H*/*L*) versus runout length, along with data of mass movements from other planetary bodies. The smaller the *H*/*L* ratio, the more mobile are the flows. Therefore, flows on Ceres are more efficient than on other planetary bodies.

extending from a hummocky area between flooded slumping blocks and propagating toward the north (Figure 4g). The cracks are of different widths and depths and are connected by shallower perpendicular ones. The central depression and the other bright spots are also affected by cracks.

3. Discussion

The occurrence of flow features indicates viscous material on the surface. The ratio between fall height and runout length (*H*/*L*) is an approximation of the coefficient of friction of sliding debris [*Schuster and Crandell*, 1984] and is useful for a comparison with flows on other planetary bodies [*De Blasio*, 2011; *McEwen*, 1989; *Moore et al*., 1999; *Singer et al*., 2012].

We used the method of *Schuster and Crandell* [1984] to determine the potential vertical drop *H* by the measuring of the relief between the top of the potential slide mass and some point in the valley below, using the HAMO DTM. For *L* we measured the probable travel distance of the flows to the end of the lobe. In Figure 5 we plot the *H*/*L* ratio of the Ceres flows as a function of runout length (a proxy for volume) along with data from other planetary bodies. The plot shows that the *H*/*L* ratio of Cerean flows is smaller, and therefore, they had to be more mobile than most mass movements and debris flows from Iapetus. Cerean runout lengths are similar to the terrestrial ones but even more mobile. Martian landslide emplacement is suggested to have about half the runout efficiency of Earth due to gravitational effects on the yield strength of materials [*McEwen*, 1989] or the absence of a lubricating pore liquid [*Brunsden*, 1979]. Similar conditions should apply on Ceres; however, flows on Ceres are more efficient than on other planetary bodies. The low values of $H/L < 0.1$ are comparable with terrestrial submarine landslides and mudflows [*Hampton et al*., 1996], as well as lava flows [*Baloga et al*., 1995], and ice flows [*Kietzig et al*., 2010]. Impact melt may also reduce the coefficient of friction within materials. Impact melt has been described on other planetary bodies, like Mars [*Carr et al*., 1977], Earth [*Osinski*, 2004], the Moon [*Bray et al*., 2010; *Shoemaker et al*., 1968], Ganymede [*Shoemaker et al*., 1982], and Vesta [*Otto et al*., 2013; *Williams et al*., 2013], as ejecta deposits with flow-like morphologies. Generally, impact melt is lobate tongues of melt rocks that normally occur at the downslope margins near the crater rim or inside craters and is similar to terrestrial lava flows [*Bray et al*., 2010; *Denevi et al*., 2012a]. Usually, impact melt is located on only one part of the crater rim but can also be asymmetrically distributed around the crater [*Stopar*, 2014]. Impact melt, as a fallback product of ejecta strictly follows gravity. It is possible that the plains and flows in Haulani, Kupalo, Ikapati, and Occator are composed of impact melt, especially the smooth lobes with well-defined margins in Haulani (Figure 1c).

On the other hand, many of the observed flows originated from distinct sources in the crater interior. In Occator and Haulani, more than one lobate flow originated close to the center and moved outward toward the walls. In Occator, these flows potentially originated from the central bright depression and appear to have moved uphill (Figures 4c and 4f). As impact melt is a fallback product, it would follow the topography and the flow fronts would have been formed in topographic lows, not higher than the source origin.

Thus, the topographic inverse behavior of flows in Occator indicates a feeding zone that pushes the flows forward by supplying low-viscosity material and a posterior collapse of the dome in the central region, possibly due to a discharge of a subsurface reservoir [*Jaumann et al*., 2016]. Furthermore, the results of *De Sanctis et al.* [2016] show that the bright spots within Occator predominantly consist of carbonates, a different material than the adjacent material, which predominantly consist of phyllosilicates. Such carbonates have also been

detected in the plumes of Enceladus [*Postberg et al*., 2011], suggesting an endogenic origin and not an impact melt origin.

Additionally, Haulani reveals multiple flow stages on the western crater flank interrupted by sharp scarps. Generally, flow-like morphologies in the ejecta are thought to be a result of either an involvement of volatiles or gases, deceleration when the ejecta motion interacts with the local topography, or post emplacement ground flow [*Boyce et al*., 2010; *Bray et al*., 2010; *Carr et al*., 1977]. A formation of multiple flow stages due to material overflowing terraces would reveal a stair stepped pattern in the profile (Figure 1h). But the overall morphology of Haulani's western crater flank shows a planar crater flanks. Liquid cryolava features can be produced by heating [*Cassen et al*., 1979] or by a release of material from a liquid subsurface layer [*Tobie et al*., 2010]. Ascent and emplacement of cryolava could be due to compositional buoyancy [*Croft et al*., 1988]. A liquid ammonia-water mixture has a similar density to water ice [*Hargitai et al*., 2014] and can be erupted by large-scale tectonic stress patterns like subsurface pressure gradients associated with topography [*Mitri et al*., 2008]. Moreover, cryolava could also be due to an overpressurization of liquid cryomagma chambers (fluid reservoirs of water ice) in an ice lithosphere [*Fagents*, 2003; *Showman et al*., 2004]. Additionally, the observation of pits in all four craters indicates a volatile rich material. On Mars and Vesta, pits are thought to be formed through degassing of volatile-bearing material heated by the impact [*Boyce et al*., 2012; *Denevi et al*., 2012b]. The pits on Ceres are also supposed to be the result of rapid postimpact outgassing of hydrated salts or ground ice [*Sizemore et al*., 2016].

Recent observations by Dawn suggest that Ceres is a weakly differentiated body with a shell dominated by an ice-rock mixture [*Fu et al*., 2015] and ammoniated phyllosilicates [*De Sanctis et al*., 2015]. Furthermore, *Neumann et al.* [2016] developed a thermal model that shows hydrated salts could be warm enough to be mobile at a depth of 1.5–5 km and could explain the buoyancy of ice and salt-enriched crustal reservoirs. Thus, impacts into such reservoir could have triggered mobility and formed cryovolcanic features, such as the flows in Occator and Haulani.

Finally, the blue color of the plains and flow materials indicates significant differences to the reddish surroundings, applying a material change. The material composing Ahuna Mons, a prominent domical feature that may be related to upwelling material, shows the same spectral characteristics as the plains and flow material, suggesting a common composition [*Ruesch et al*., 2016; *Zambon et al*., 2016]. *Ruesch et al.* [2016] suppose that Ahuna Mons is composed of subsurface material. This supports the assumption that plains and flow materials also originate from the subsurface and their release is triggered by impact [*Jaumann et al*., 2016]. Although no water ice has been detected by VIR (Visible and Infrared Spectrometer) in the vicinity of the discussed impact craters so far, it is still possible that water ice existed but sublimated quickly after being exposed at the surface and might have caused the bluish color [*Stephan et al*., 2016]. However, also differences in the grain size of phyllosilicates are in discussion to cause the blue color [*Jaumann et al*., 2016; *Stephan et al*., 2016]. Extremely fine-grained ejecta material redeposited during the impact events could also explain the smooth surfaces of the observed flow features.

Age determinations indicate that the bluish material is mainly associated with the youngest impact craters on Ceres [*Schmedemann et al*., 2016]. Thus, the bluish craters seem to be one of the youngest geologic features on Ceres.

4. Conclusion

The compositional differences of the observed flows, and their discrete feeding sources, suggest a cryovolcanic origin. The correlation of such flow features with impact craters indicates an impact triggered release of subsurface material or hydrothermal processes triggered by impact heat. Crustal material enriched in hydrated salts, either as part of a subsurface layer or accumulated in smaller local reservoirs within the crust at different depths, could be mobilized by tectonic weakening and/or by impacts. Another possible emplacement scenario is the formation of subsurface reservoirs enriched in salt-bearing components driven upward by density/temperature inhomogeneity. A possible example for such a mechanism is the tectonic structure at the southern part of Occator, where a pattern of cracks indicates breaking of the plains material by upwelling and the partly polygonal arrangements suggest formation by dehydration. Although we see impact melt structures, e.g., smooth well-defined flows around Haulani, Ikapati, and Kupalo, the plains in Occator and the viscous flows on Haulani's western crater flank are more likely the result of impact triggered cryovolcanic

activity. Impacts hitting the surface above subsurface reservoirs enriched with hydrated salts will mobilize these compounds, produce additional hydration of salts, and release them as flows. The observed craters may have tapped into salt-rich crustal reservoirs, triggering the mobility of material and formed the cryovolcanic features. The material might have sustained long after the impact, as indicated by the significantly younger age of the plains and flow materials.

Thus, due to the similarity of impact melt structures and cryolava flows, we assume that we have a coexistence of both types on Ceres.

Acknowledgments
We thank the Dawn team for the development, cruise, orbital insertion, and operations of the Dawn spacecraft at Ceres. Portions of this work were performed at the DLR Institute of Planetary Research, at the Jet Propulsion Laboratory (JPL) under contract with NASA. Dawn data are archived with the NASA Planetary Data System (http://sbn.pds.nasa.gov/). K. Krohn is supported by the Helmholtz Association (HGF) through the research Helmholtz Postdoc Program.

References

Baloga, S., P. D. Spudis, and J. E. Guest (1995), The dynamics of rapidly emplaced terrestrial lava flows and implications for planetary volcanism, *J. Geophys. Res.*, *100*, 24,509–24,519, doi:10.1029/95JB02844.
Boyce, J. M., N. Barlow, P. Mouginis-Mark, and S. Stewart (2010), Rampart craters on Ganymede: Their implications for fluidized ejecta emplacement, *Meteor. Planet. Sci.*, *45*, 638–661.
Boyce, J. M., L. Wilson, P. J. Mouginis-Mark, C. W. Hamilton, and L. L. Tornabene (2012), Origin of small pits in Martian impact craters, *Icarus*, *221*(1), 262–275.
Bray, V. J., et al. (2010), New insight into lunar impact melt mobility from the LRO camera, *Geophys. Res. Lett.*, *37*, L21202, doi:10.1029/2010GL044666.
Brunsden, D. (1979), Mass movements, in *Process in Geomorphology*, edited by C. E. Embleton and J. B. Thornes, pp. 130–186, Edward Arnold, London.
Carr, M. H., L. S. Crumpler, J. A. Cutts, R. Greeley, J. E. Guest, and H. Masursky (1977), Martian impact craters and emplacement of ejecta by surface flow, *J. Geophys. Res.*, *82*, 4055–4065, doi:10.1029/JS082i028p04055.
Cassen, P., R. T. Reynolds, and S. J. Peale (1979), Is there liquid water on Europa, *Geophys. Res. Lett.*, *6*, 731–734, doi:10.1029/GL006i009p00731.
Castillo-Rogez, J. C., and T. B. McCord (2010), Ceres' evolution and present state constrained by shape data, *Icarus*, *205*, 443–459.
Croft, S. K., J. I. Lunine, and J. Kargel (1988), Equation of state of ammonia-water liquid: Derivation and planetological applications, *Icarus*, *73*, 279–293.
De Blasio, F. V. (2011), *Introduction to the Physics of Landslides*, 1st ed., Springer, Netherlands.
De Sanctis, M. C., et al. (2015), Ammoniated phyllosilicates with a likely outer Solar System origin on (1) Ceres, *Nature*, *528*, 241–244.
De Sanctis, M. C., et al. (2016), Bright carbonate deposits as evidence of aqueous alteration on (1) Ceres, *Nature*, *53*, 54–57.
Denevi, B. W., et al. (2012a), Physical constraints on impact melt properties from Lunar Reconnaissance Orbiter Camera images, *Icarus*, *219*, 665–675.
Denevi, B. W., et al. (2012b), Pitted terrain on Vesta and implications for the presence of volatiles, *Science*, *338*, 246–249.
Fagents, S. A. (2003), Considerations for effusive cryovolcanism on Europa: The post-Galileo perspective, *J. Geophys. Res.*, *108*(E12), 5139, doi:10.1029/2003JE002128.
Fu, R. R., A. Ermakov, M. T. Zuber, and H. H. Bradford (2015), The global scale relaxation state of Ceres, paper presented at AGU Fall Meeting.
Hampton, M. A., H. J. Lee, and J. Locat (1996), Submarine landslides, *Rev. Geophys.*, *34*, 33–59, doi:10.1029/95RG03287.
Hargitai, H., Á. Kereszturi, and M. Choukroun (2014), Cryovolcanic features, in *Encyclopedia of Planetary Landforms*, edited by H. Hargitai and Á. Kereszturi, pp. 1–10, Springer, New York.
Jaumann, R., et al. (2016), Age-dependent morphological and compositional variations on Ceres, Proc. Lunar Planet. Sci. Conf. 47th, p. 1455.
Kietzig, A.-M., S. G. Hatzikiriakos, and P. Englezos (2010), Physics of ice friction, *J. Appl. Phys.*, *107*, 081101, doi:10.1063/1.3340792.
Krohn, K., et al. (2016), Channels and cryogenic flow features on Ceres, Proc. Lunar Planet. Sci. Conf., p. 2001.
McCord, T. B., and C. Sotin (2005), Ceres: Evolution and current state, *J. Geophys. Res.*, *110*, E05009, doi:10.1029/2004JE002244.
McCord, T. B., J. Castillo-Rogez, and A. Rivkin (2011), Ceres: Its origin, evolution and structure and Dawn's potential contribution, *Space Sci. Rev.*, *163*, 63–76.
McEwen, A. S. (1989), Mobility of large rock avalanches: Evidence from Valles Marineris, Mars, *Geology*, *17*, 1111–1114.
Mitri, G., A. P. Showman, J. I. Lunine, and R. M. C. Lopes (2008), Resurfacing of Titan by ammonia-water cryomagma, *Icarus*, *196*, 216–224.
Moore, J. M., et al. (1999), Mass movement and landform degradation on the icy Galilean satellites: Results of the Galileo nominal mission, *Icarus*, *140*, 294–312.
Nathues, A., et al. (2015), Sublimation in bright spots on (1) Ceres, *Nature*, *528*, 237–240.
Neesemann, A., T. Kneissl, N. Schmedemann, S. H. G. Walter, G. G. Michael, S. van Gasselt, H. Hiesinger, R. Jaumann, C. Raymond, and C. T. Russell (2016), Size-frequency distributions of km to sub-km sized impact craters on Ceres, Proc. Lunar Planet. Sci. Conf, p. 2936.
Neumann, W. O., D. Breuer, and T. Spohn (2016), Differentiation of Ceres and her present-day thermal state, Proc. Lunar and Planetary Science Conference, p. 2307.
Osinski, G. R. (2004), Impact melt rocks from the Ries structure, Germany: An origin as impact melt flows?, *Earth Planet. Sci. Lett.*, *226*, 529–543.
Otto, K., et al. (2013), Mass wasting features in Vesta's south polar basin Rheaslilvia, *J. Geophys. Res. Planets*, *118*, 2279–2294, doi:10.1002/2013JE004333.
Pieters, C. M., et al. (2016), Surface processes and space weathering on Ceres, Proc. Lunar Planet. Sci. Conference, p. 1383.
Postberg, F., J. Schmidt, J. Hillier, S. Kempf, and R. Srama (2011), A salt-water reservoir as the source of a compositionally stratified plume on Enceladus, *Nature*, *474*, 620–622.
Preusker, F., F. Scholten, K.-D. Matz, S. Elgner, R. Jaumann, T. Roatsch, S. P. Joy, C. A. Polanskey, C. A. Raymond, and C. T. Russell (2016), Dawn at Ceres—Shape model and rotational state, Proc. Lunar and Planetary Science Conference, p. 1954.
Rivkin, A. S., J.-Y. Li, R. E. Milliken, L. F. Lim, A. J. Lovell, B. E. Schmidt, L. A. McFadden, and B. A. Cohen (2011), The surface composition of Ceres, *Space Sci. Rev.*, *163*, 95–116.
Ruesch, O., et al. (2016), Ahuna Mons: A geologically-young extrusive dome on Ceres, Proc. Lunar Planet. Sci. Conf., p. 2279.
Russell, C. T., and C. A. Raymond (2011), The Dawn mission to Vesta and Ceres, *Space Sci. Rev.*, *163*, 3–23.
Russell, C. T., et al. (2015), Dawn arrives at Ceres: Results of the survey orbit, European Planet. Sci. Congress, 10.
Schmedemann, N., R. J. Wagner, G. Michael, B. A. Ivanov, T. Kneissl, A. Neesemann, H. Hiesinger, R. Jaumann, C. A. Raymond, and C. T. Russell (2016), Crater scaling on weak targets, from Ceres to Icy satellites, Proc. Lunar Planet. Sci. Conf., p. 2236.

Schuster, R. L., and D. R. Crandell (1984), Catastrophic debris avalanches from volcanoes, paper presented at IV International Symposium on Landslide Proceedings, Toronto.
Shoemaker, E. M., R. M. Batson, H. E. Holt, E. C. Morris, J. J. Rennilson, and E. A. Whitaker (1968), Television observations from Surveyor 3, *J. Geophys. Res.*, *73*, 3989–4043, doi:10.1029/JB073i012p03989.
Shoemaker, E. M., B. K. Lucchitta, D. E. Wilhelms, J. B. Plescia, and S. W. Squyres (1982), The geology of Ganymede, in *Satellites of Jupiter*, edited by D. Morrison, pp. 435–520, Univ. of Arizona Press, Tucson, Ariz.
Showman, A. P., I. Mosqueira, and J. W. Head (2004), On the resurfacing of Ganymede by liquid water volcanism, *Icarus*, *172*, 625–640.
Sierks, H., et al. (2011), The Dawn Framing Camera, *Space Sci. Rev.*, *163*, 263–327.
Singer, K. N., W. B. McKinnon, P. M. Schenk, and J. M. Moore (2012), Massive ice avalanches on Iapetus mobilized by friction reduction during flash heating, *Nat. Geosci.*, *5*(8), 574–578.
Sizemore, H. G., et al. (2016), Preliminary constraints on the volumetric concentration of shallow ground Ice on Ceres from geomorphology, Proc. Lunar and Planetary Science Conference, p. 1628.
Stephan, K., et al. (2016), The nature of Ceres' bluish material, AGU Fall Meeting Abstracts, 43, 2122.
Stopar, J. D. (2014), Impact melt flows, in *Encyclopedia of Planetary Landforms*, edited by H. Hargitai and Á. Kereszturi, pp. 1–9, Springer, New York.
Thomas, P. C., J. W. Parker, L. A. McFadden, C. T. Russell, S. A. Stern, M. V. Sykes, and E. F. Young (2005), Differentiation of the asteroid Ceres as revealed by its shape, *Nature*, *437*, 224–226.
Tobie, G., et al. (2010), Surface, subsurface and atmosphere exchanges on the satellites of the outer Solar System, *Space Sci. Rev.*, *153*, 375–410.
Williams, D. A., et al. (2013), Lobate and flow-like features on asteroid Vesta, *Planet. Space Sci.*, *103*, 24–35.
Zambon, F., et al. (2016), Mineralogy of Ahuna Mons, paper presented at DPS 48/EPSC 11, Pasadena, Calif.